Supporting Information

for

Boronate-appended polymers with diol-functionalized ferrocene: an effective and selective system for voltammetric glucose sensing

Jakub P. Sęk,[a] Sabina Kaczmarczyk,[a] Katarzyna Guńka,[b] Agata Kowalczyk,*[a] Krzysztof M. Borys,[b] Artur Kasprzak*[b] and Anna M. Nowicka*[a]

[a]Faculty of Chemistry, University of Warsaw, Pasteura 1 Str., PL-02-093 Warsaw, Poland
[b]Faculty of Chemistry, Warsaw University of Technology, Noakowskiego 3 Str., PL-00-664 Warsaw, Poland

*Corresponding authors: Agata Kowalczyk (akowalczyk@chem.uw.edu.pl), Anna M. Nowicka (anowicka@chem.uw.edu.pl), Artur Kasprzak (akasprzak@ch.pw.edu.pl)

1. NMR data

Note: Because of solubility issues, the spectra were measured in D_2O or CD_3OD in order to acquire good quality NMR spectra. Due to a significant broadening of the peaks coming from PAMAM and PEI, as well as peaks overlapping, the signals coming from PEI and PAMAM have not been integrated. The given integrals should be treated as approximate ones.

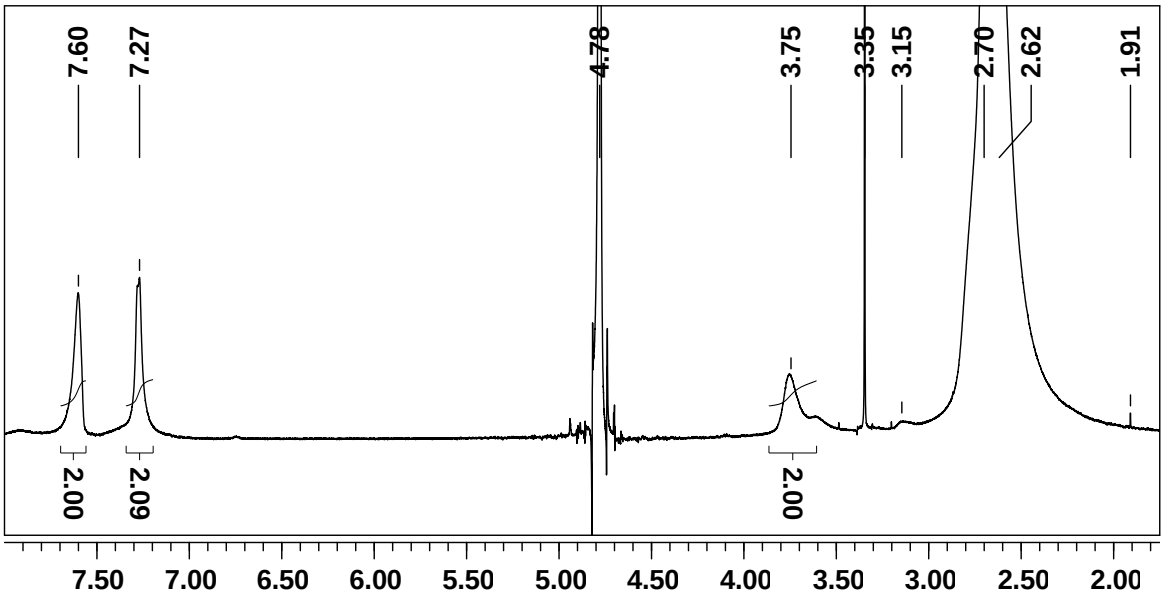

Figure S1. ^{1}H NMR spectrum (500 MHz, D_2O) of **PEI-B(OH)$_2$**.

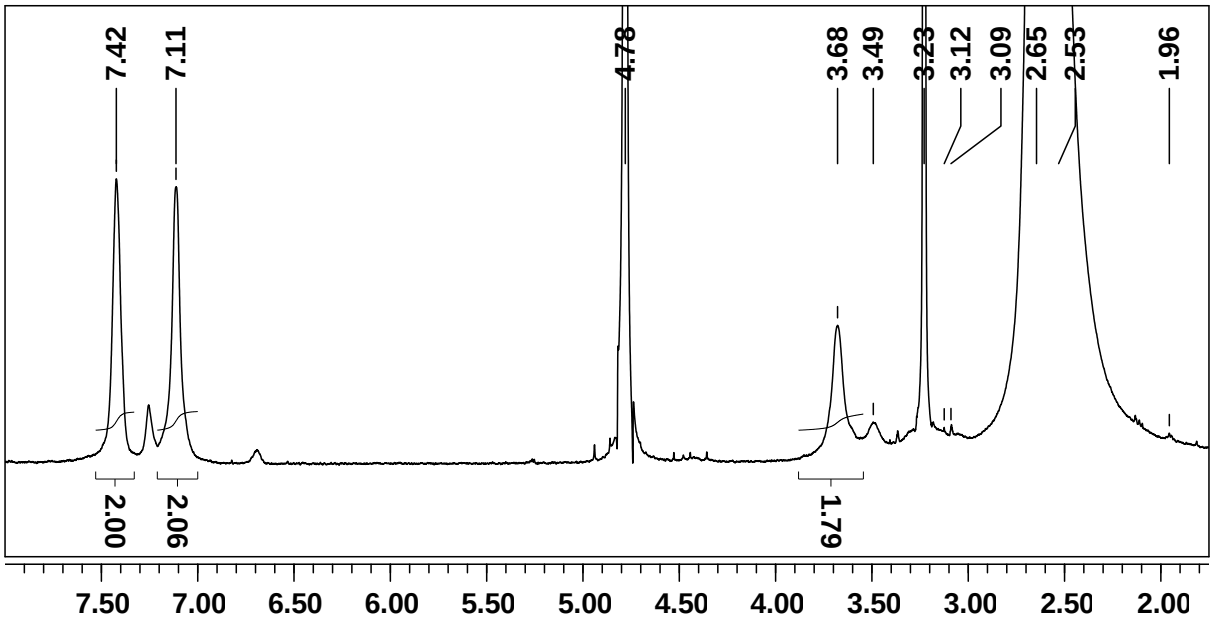

Figure S2. ^{1}H NMR spectrum (500 MHz, CD_3OD) of **PEI-B(OH)$_2$**.

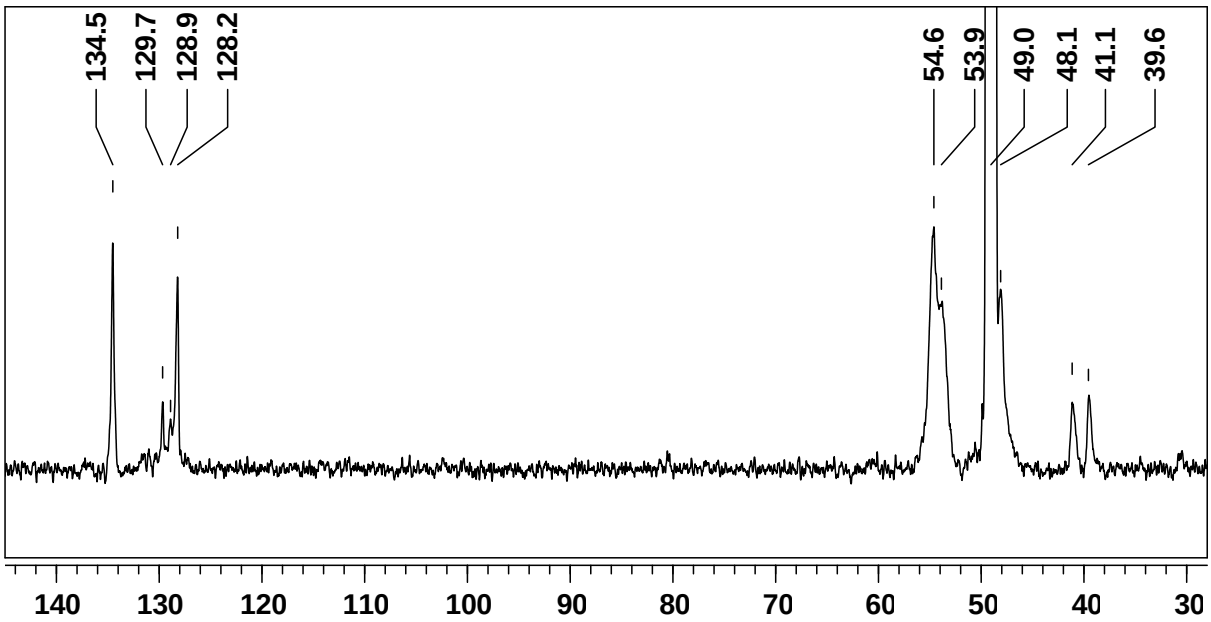

Figure S3. ^{13}C NMR spectrum (125 MHz, CD_3OD) of **PEI-B(OH)$_2$**.

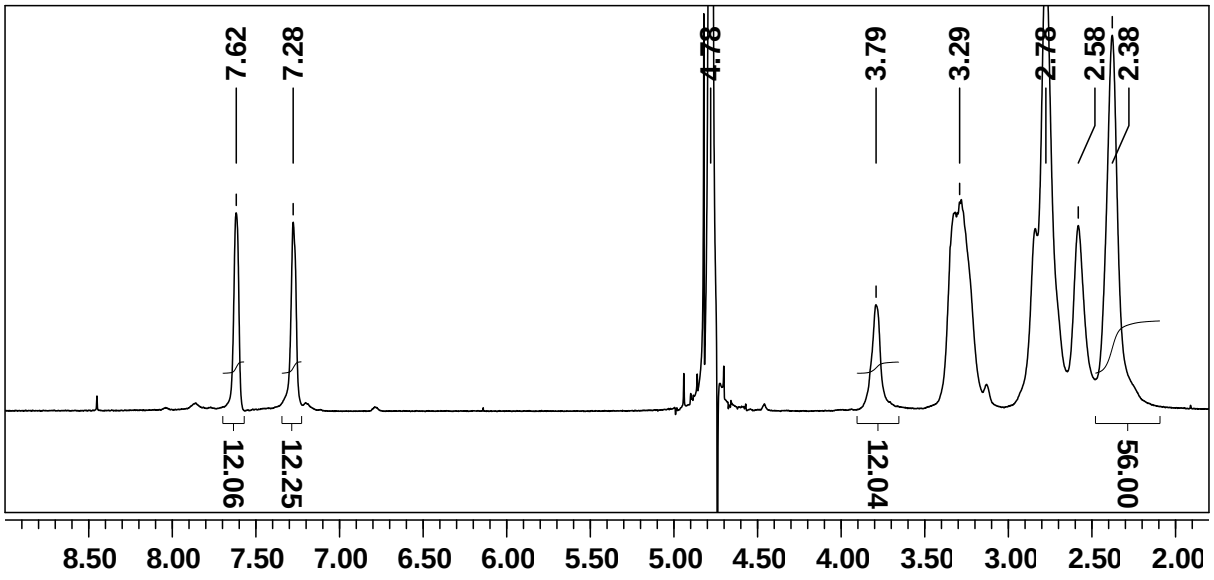

Figure S4. ^{1}H NMR spectrum (500 MHz, D_2O) of **PAMAM-1-B(OH)$_2$**.

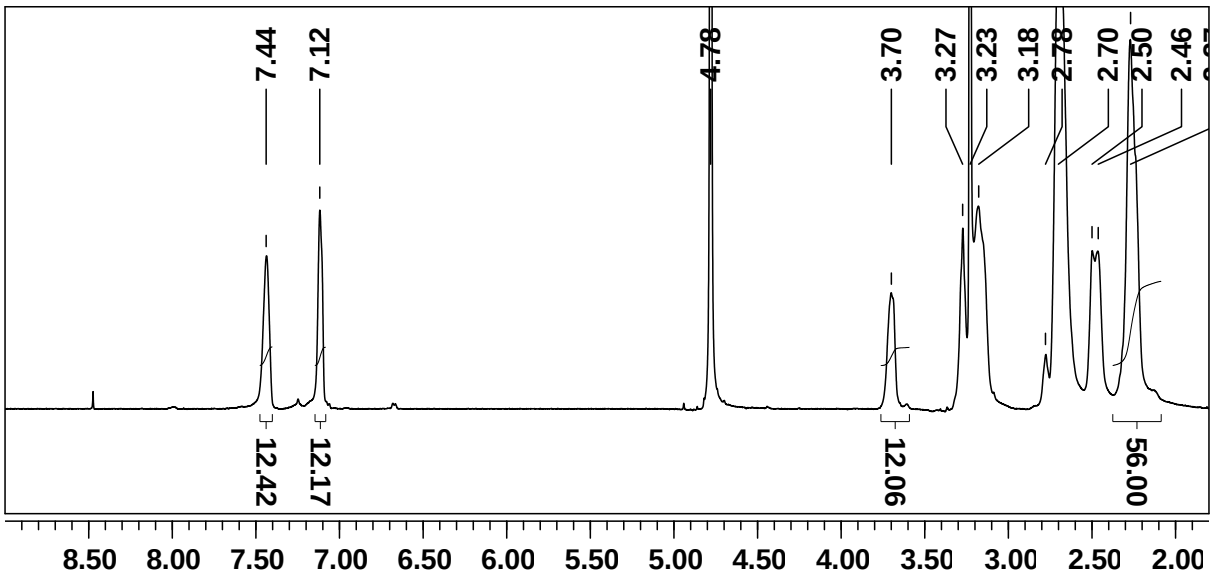

Figure S5. ^{1}H NMR spectrum (500 MHz, CD_3OD) of **PAMAM-1-B(OH)$_2$**.

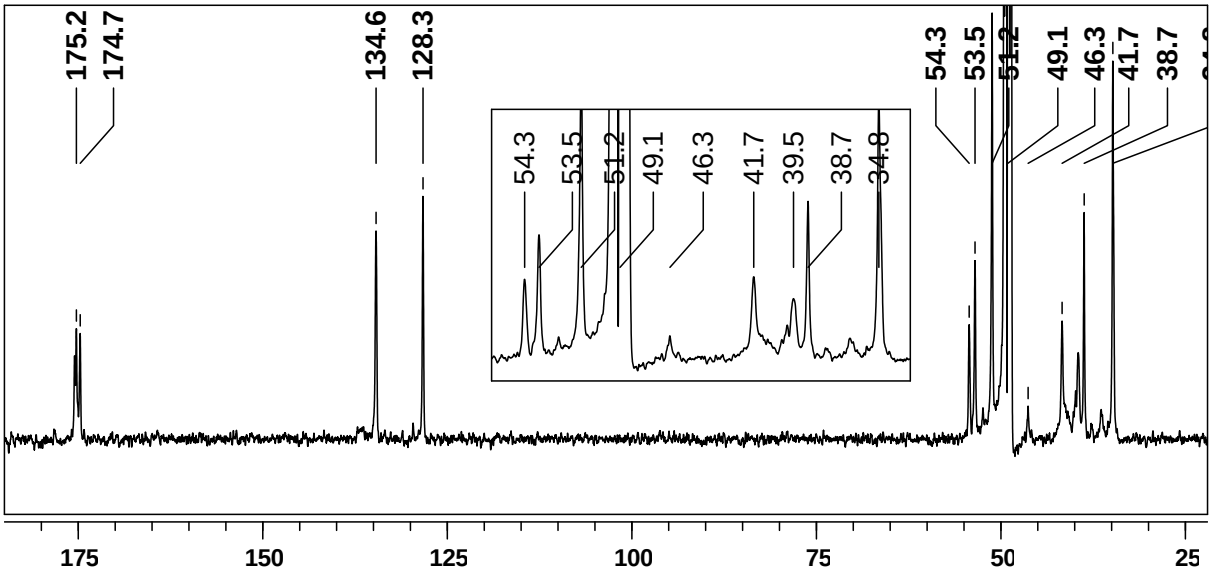

Figure S6. ^{13}C NMR spectrum (125 MHz, CD_3OD) of **PAMAM-1-B(OH)$_2$**.

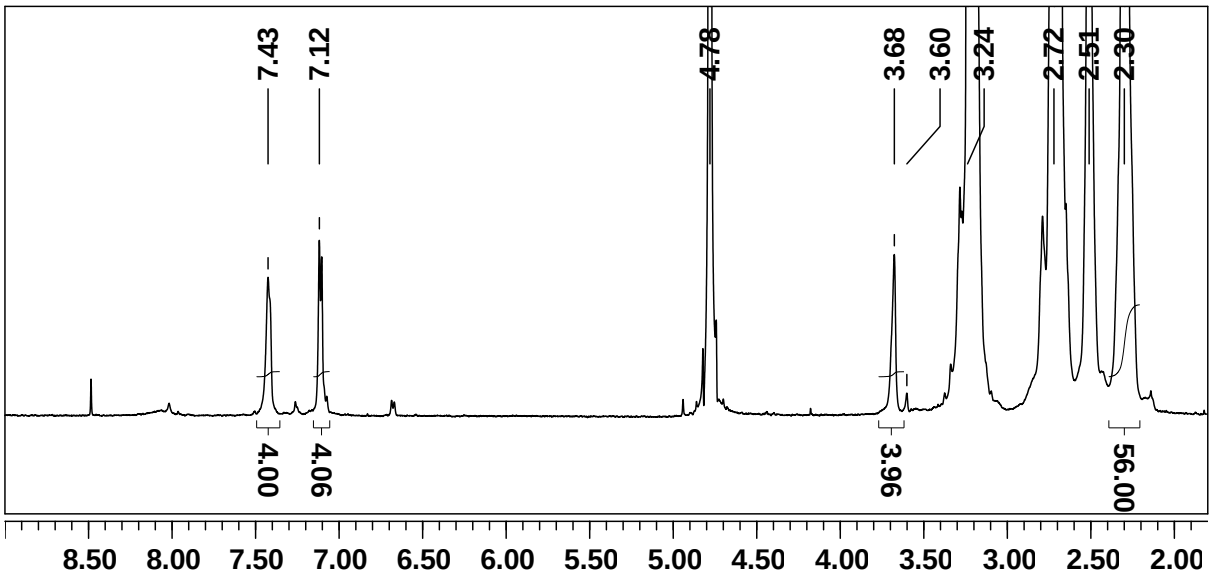

Figure S7. ^{1}H NMR spectrum (500 MHz, CD_3OD) of **PAMAM-2-B(OH)$_2$**.

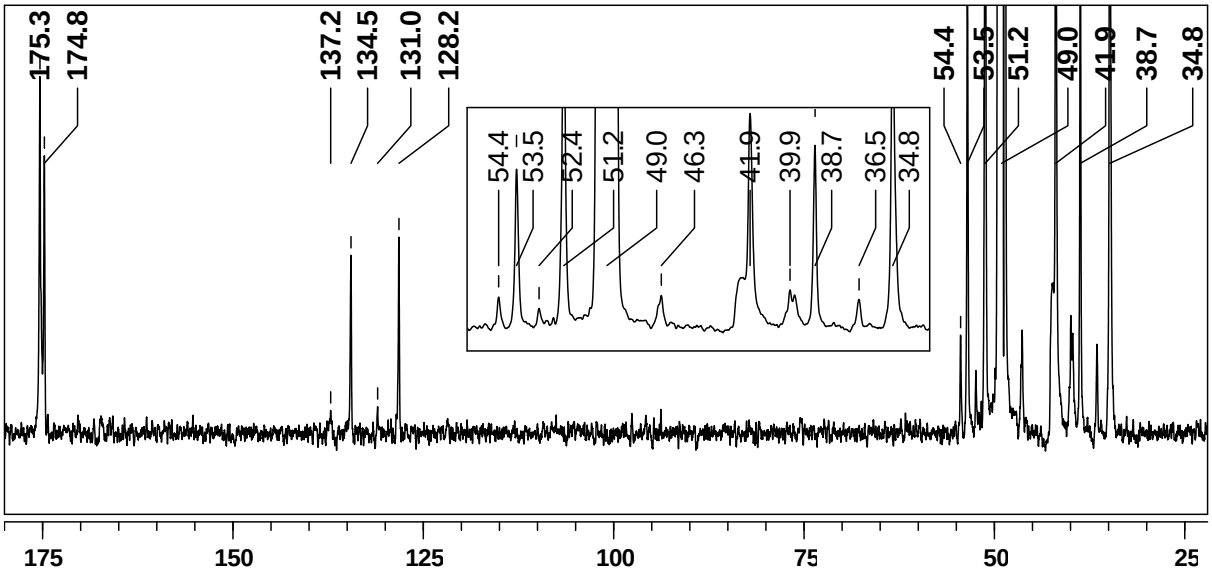

Figure S8. ^{13}C NMR spectrum (125 MHz, CD_3OD) of **PAMAM-2-B(OH)$_2$**.

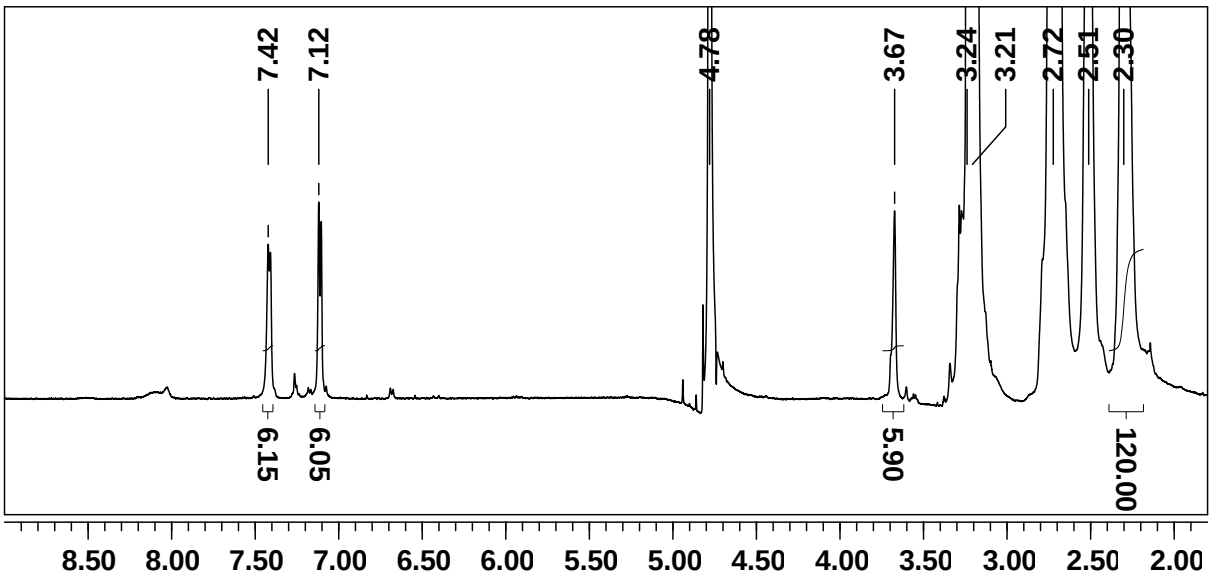

Figure S9. ^{1}H NMR spectrum (500 MHz, CD_3OD) of **PAMAM-3-B(OH)$_2$**.

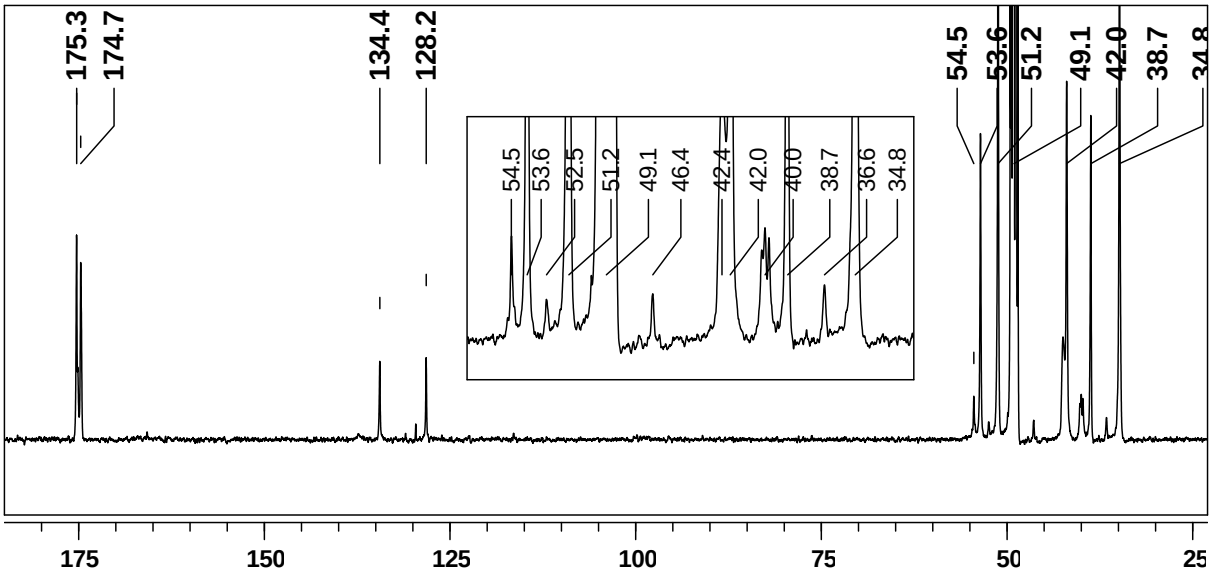

Figure S10. ^{13}C NMR spectrum (125 MHz, CD_3OD) of **PAMAM-3-B(OH)$_2$**.

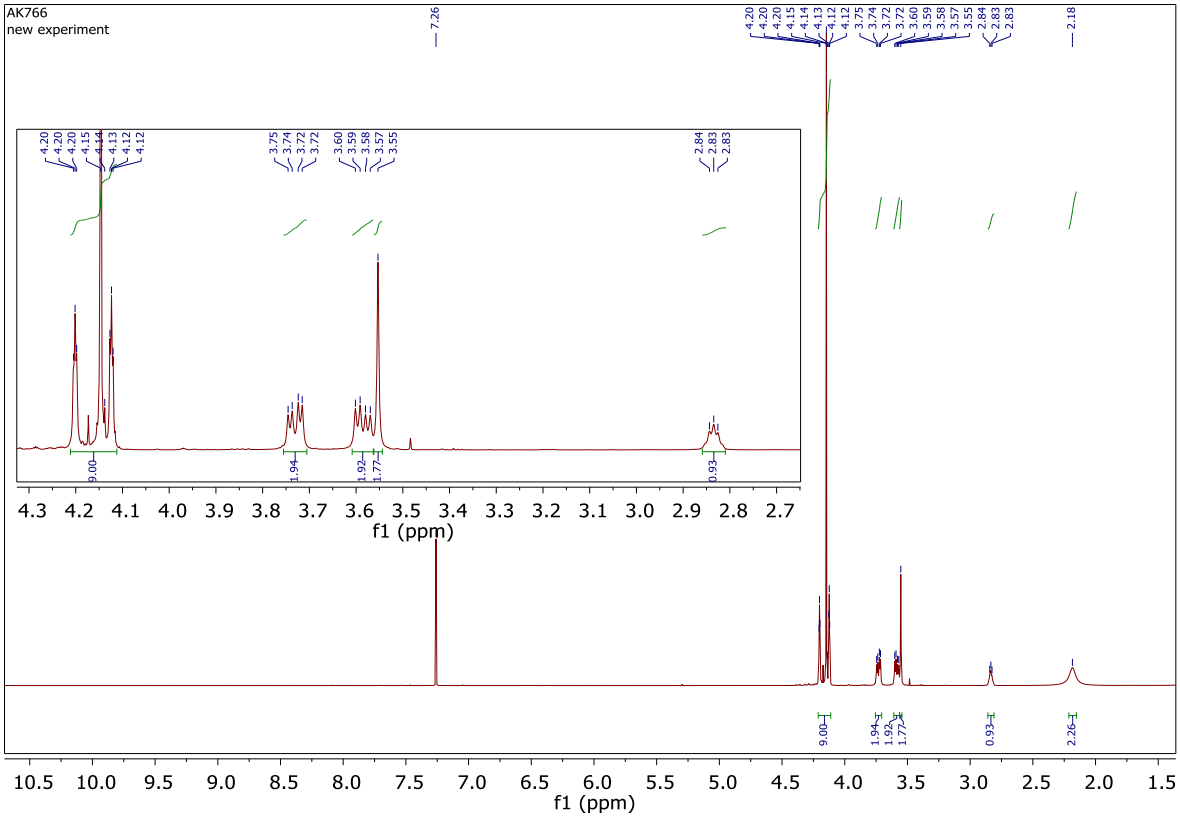

Figure S11. ^{1}H NMR spectrum (500 MHz, $CDCl_3$) of Fc-1,3-diol.

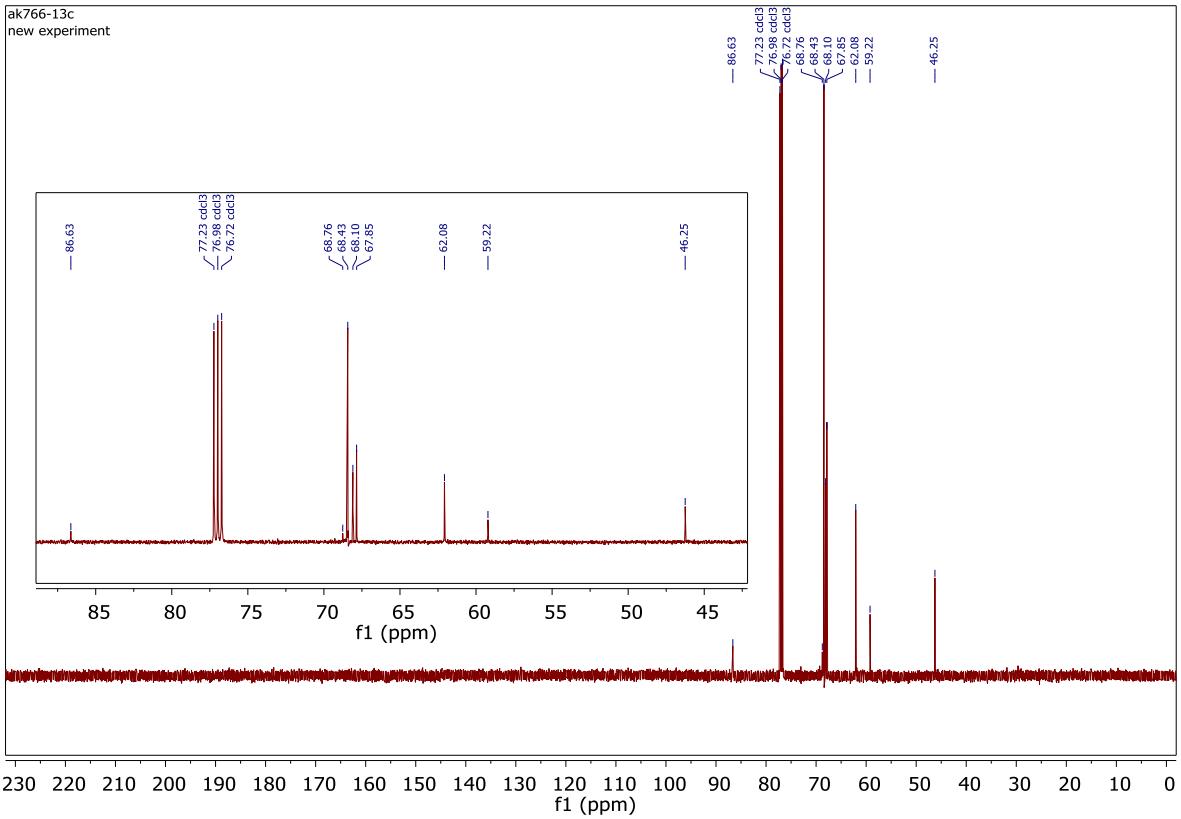

Figure S12. ^{13}C NMR spectrum (125 MHz, $CDCl_3$) of Fc-1,3-diol.

Table S1. NMR data for the PEI and PAMAM derivatives.

PEI-B(OH)$_2$	^{1}H NMR δ_H (500 MHz, D_2O, ppm):	7.57-7.63 (bm, 2H), 7.24-7.30 (bm, 2H), 3.70-3.80 (bs, 2H), 3.17-3.13 (bm, PEI) 2.50 – 2.80 (bm, PEI)
	^{1}H NMR δ_H (500 MHz, CD_3OD, ppm):	7.40-7.45 (bm, 2H), 7.07-7.15 (bm, 2H), 3.62-3.72 (bs, 2H), 3.12 – 3.09 (bm, PEI) 2.40-2.70 (bm, PEI)
	^{13}C NMR δ_C (125 MHz, CD_3OD, ppm):	134.5; 129.7; 128.9; 128.2; 54.6; 53.9; 48.1; 41.1; 39.6
PAMAM-2-B(OH)$_2$	^{1}H NMR δ_H (500 MHz, D_2O, ppm):	8.45 (s), 7.57-7.60 (bm, 4H), 7.24-7.27 (bm, 4H), 3.73-3.78 (bs, 4H), 3.25-3.31 (bm, PAMAM), 2.75-2.85 (bm, PAMAM), 2.68-2.72 (bm, PAMAM), 2.57-2.65 (bm, PAMAM), 2.35-2.45 (bm, PAMAM)
	^{1}H NMR δ_H (500 MHz, CD_3OD, ppm):	8.48 (s), 7.40-7.45 (bm, 4H), 7.15-7.10 (bm, 4H), 3.60-3.72 (bs, 4H), 3.14-3.34 (bm, PAMAM), 2.60-2.80 (bm, PAMAM), 2.45-2.55 (bm, PAMAM), 2.20-2.40 (bm, PAMAM)
	^{13}C NMR δ_C (125 MHz, CD_3OD, ppm):	175.3; 174.8; 137.2; 134.5; 131.0; 128.2; 54.4; 53.5; 51.2; 41.9; 38.7; 34.8
PAMAM-1-B(OH)$_2$	^{1}H NMR δ_H (500 MHz, D_2O, ppm):	7.67-7.58 (bm, 12H), 7.32-7.23 (bm, 4H), 3.85-3.71 (bs, 12H), 3.39-3.19 (bm, PAMAM), 2.88-2.68 (bm, PAMAM), 2.60-2.53 (bm, PAMAM), 2.45-2.35 (bm, PAMAM)
	^{1}H NMR δ_H (500 MHz, CD_3OD, ppm):	7.40-7.48 (bm, 12H), 7.10-7.16 (bm, 12H), 3.65-3.75 (bs, 12H), 3.37-3.08 (bm, PAMAM), 2.78-2.74 (bm, PAMAM), 2.55-2.40 (bm, PAMAM), 2.25-2.40 (bm, PAMAM)
	^{13}C NMR δ_C (125 MHz, CD_3OD, ppm):	175.2; 174.7; 134.6; 128.3; 54.3; 53.5; 51.2; 46.3; 41.7; 38.7; 34.8
PAMAM-3-B(OH)$_2$	^{1}H NMR δ_H (500 MHz, D_2O, ppm):	7.58-7.63 (bm, 6H), 7.25-7.30 (bm, 6H), 3.73-3.79 (bs, 6H), 3.19-3.35 (bm, PAMAM), 2.71-2.89 (bm, PAMAM), 2.60-2.68 (bm, PAMAM), 2.40-2.46 (bm, PAMAM)
	^{1}H NMR δ_H (500 MHz, CD_3OD, ppm):	7.40-7.45 (bm, 6H), 7.11-7.16 (bm, 6H), 3.65-3.70 (bs, 6H), 3.11-3.34 (bm, PAMAM), 2.70-2.86 (bm, PAMAM), 2.51-2.60 (bm, PAMAM), 2.25-2.38 (bm, PAMAM)
	^{13}C NMR δ_C (125 MHz, CD_3OD, ppm):	175.3; 174.7; 134.4; 128.2; 54.5; 53.6; 51.2; 46.4; 42.0; 40.0; 38.7; 36.6; 34.8

Table S2. Detailed data for the synthesis and purification of PEI derivatives.

	PEI-B(OH)$_2$
(1) PEI mass/ mg	500
(2) MeOH volume/ mL	20
(3) 4-FPBA quantity / mmol / mg	1.2 / 180
(4) $NaBH_4$ quantity/ mmol / mg	4.8 / 182
(5) Sample volume for dialysis / mL	20
(6) Dialysis time/ days	5
(7) Dialysis sack used / kDa	1
(8) Product mass/ mg	458

Table S3. Detailed data for the synthesis and purification of PAMAM derivatives.

	PAMAM-2-B(OH)$_2$	**PAMAM-1-B(OH)$_2$**	**PAMAM-3-B(OH)$_2$**
(1) 2- or 3-generation PAMAM mass/ mg	350	350	350
(2) MeOH volume/ ml	14	14	14
(3) 4-FPBA quantity/ mmol / mg	0.2 / 32	0.86 / 129	0.2 / 31
(4) $NaBH_4$ quantity/ mmol / mg	0.8 / 33	3.4 / 130	0.8 / 31
(5) Sample volume for dialysis / mL	20	25	25
(6) Dialysis time/ days	1	1	1
(7) Dialysis sack used / kDa	2	2	2
(8) Product mass / mg	241	368	378
Modification level PAMAM	16 : 2	16 : 8	32 : 4

2. Interactions between phenylboronic acid (PBA) and Fc-1,3-diol

At first, the interactions between phenylboronic acid (PBA) and Fc-1,3-diol, a redox probe aimed to be used for the sensor construction, were probed spectroscopically with ^{1}H NMR (Figure S13). Basically, the NMR samples consisted of different amounts of PBA and Fc-1,3-diol. The formation of boronate ester between these molecules has been confirmed by four major factors: (i) the disappearance of OH signals coming from PBA at *ca*. 8.01 ppm; (ii) disappearance of the OH signals coming from the Fc-1,3-diol at *ca*. 4.43 ppm; (iii) the presence of new peaks coming from the aromatic protons of the boronate ester at *ca*. 7.66 ppm; (iv) shifting of the signals coming from the Fc-1,3-diol and the change in their multiplicity. It is worth to note that the formation of the boronate ester in this experiment is a dynamic process, therefore, for some samples with the excess of PBA, the peaks coming from free PBA were observed (see Figure S13 B).

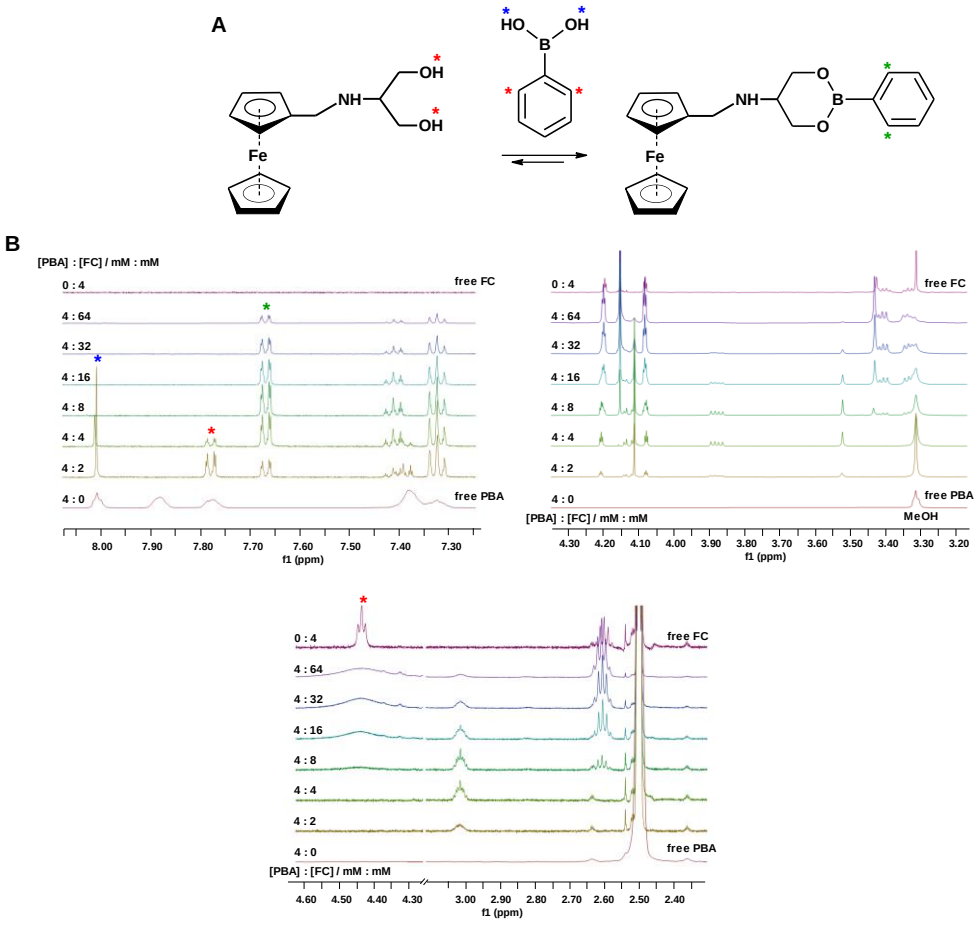

Figure S13. (A) Boronate ester formation between phenylboronic acid (PBA) and Fc-1,3-diol (FC); (B) evolution of NMR spectra for the different mixtures of phenylboronic acid and Fc-1,3-diol (selected insets are presented and the crucial features standing for the formation of the boronate ester are marked with stars).

3. Affinity of phenylboronic systems to Fc-1,3-diol and glucose

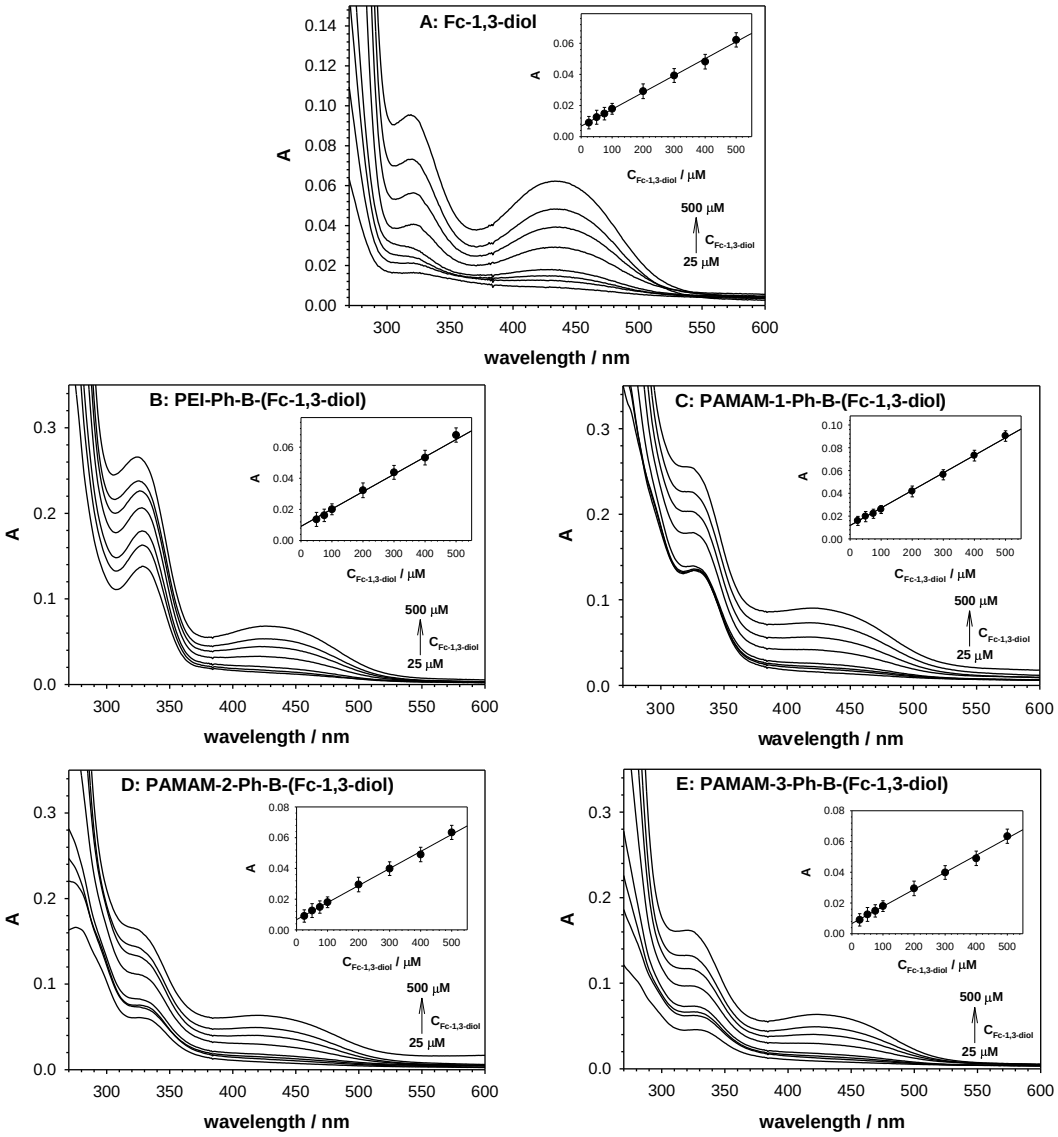

Figure S14. UV-vis spectra of Fc-1,3-diol (A) and its complexes with PEI-Ph-B(OH)$_2$ (B), PAMAM-1-Ph-B(OH)$_2$ (C), PAMAM-2-Ph-B(OH)$_2$ (D) and PAMAM-3-Ph-B(OH)$_2$ (E) recorded in 0.02 M PBS buffer, pH 7.4 with addition of 5% DMSO. Insets: Dependence of absorbance at 430 nm *versus* Fc-1,3-diol. Experimental conditions: $C_{Fc\text{-}1,3\text{-}diol}$ = 25-500 μM; $C_{R\text{-}Ph\text{-}B(OH)_2}$ = 0.25 mg·mL^{-1}.

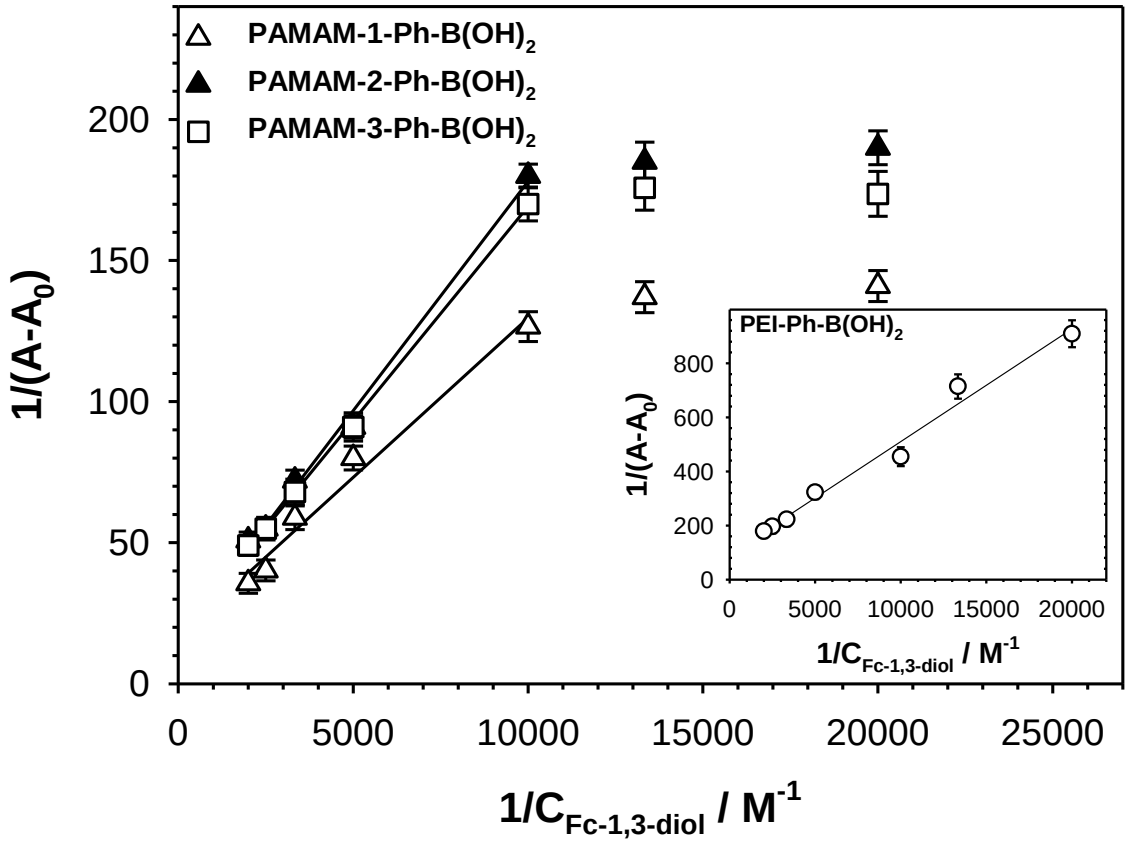

Figure S15. Benesi-Hildebrand plots for the complexes of Fc-1,3-diol and R-Ph-B(OH)$_2$ receptors. Experimental conditions as in Figure 1.

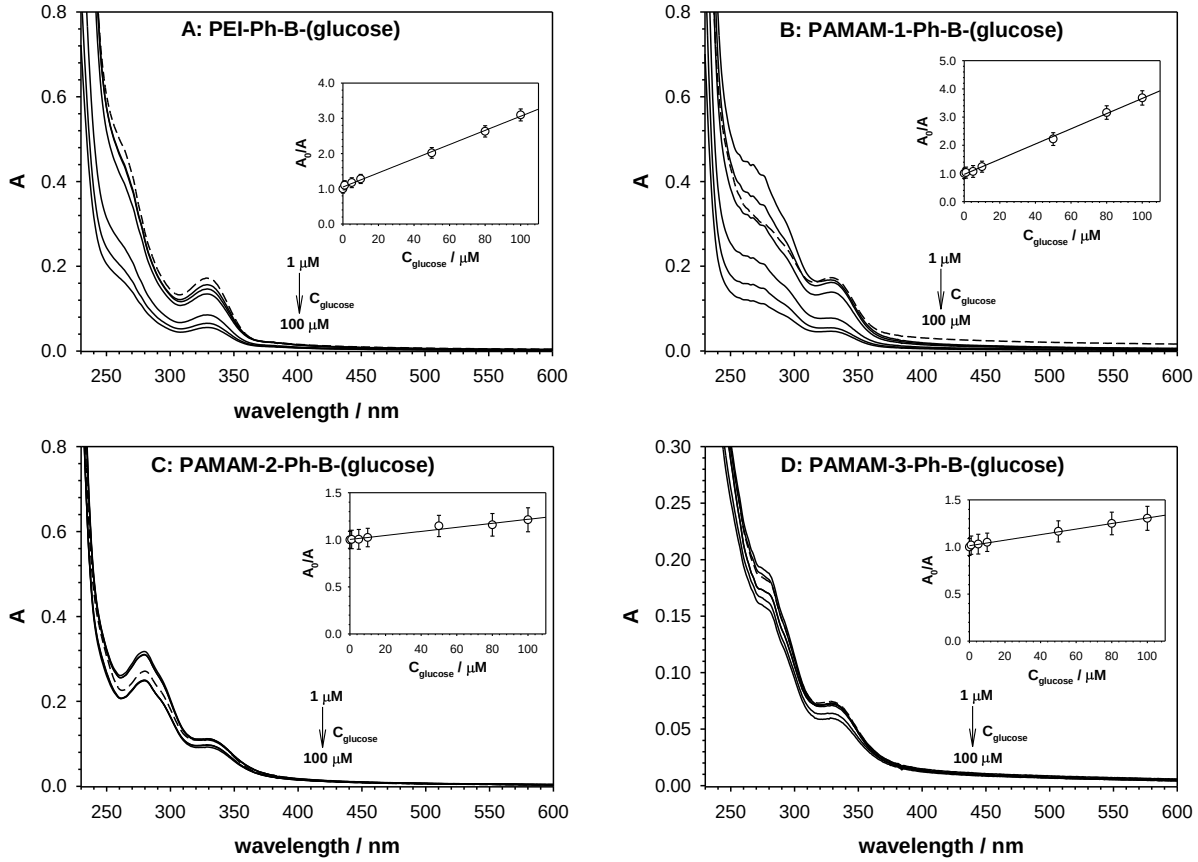

Figure S16. UV-vis spectra of glucose complexes with PEI-Ph-B(OH)$_2$ (A), PAMAM-1-Ph-B(OH)$_2$ (B), PAMAM-2-Ph-B(OH)$_2$ (C) and PAMAM-3-Ph-B(OH)$_2$ (D) recorded in 0.02 M PBS buffer, pH 7.4, with addition of 5% DMSO. Insets: Stern-Volmer dependences. Experimental conditions: $C_{glucose}$ = 1-100 μM; $C_{R\text{-}Ph\text{-}B(OH)_2}$ = 0.25 mg·mL^{-1}; dashed lines: spectra of pure R-Ph-B(OH)$_2$ receptors.

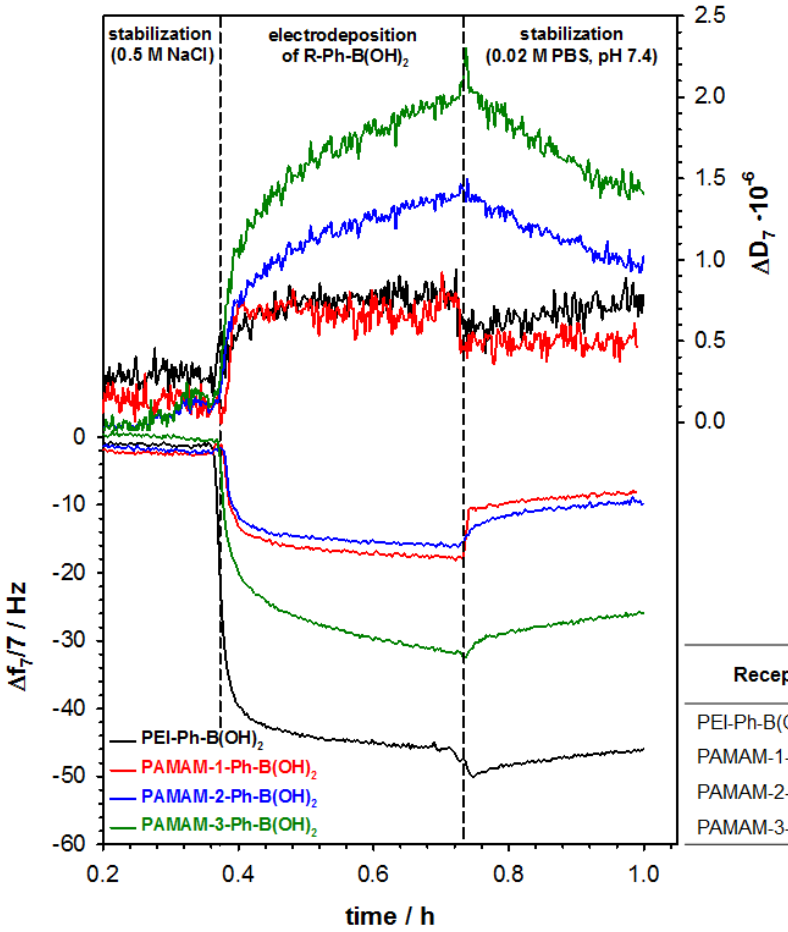

Receptor layer	*Thickness* [nm]	$\Delta D_7/\Delta f_7 \cdot 10^9$ [Hz^{-1}]
PEI-Ph-B(OH)$_2$	4.7±0.3	16.6±0.9
PAMAM-1-Ph-B(OH)$_2$	3.2±0.2	42.6±1.6
PAMAM-2-Ph-B(OH)$_2$	3.1±0.2	85.4±3.9
PAMAM-3-Ph-B(OH)$_2$	4.9±0.5	62.9±2.5

Figure S17. Typical QCM-D spectra of the shifts in frequency and dissipation factor recorded during formation of R-Ph-B(OH)$_2$ layers. Experimental conditions: 0.5 M NaCl, $C_{\text{R-Ph-B(OH)}_2}$ = 0.25 mg·mL^{-1}.